Supporting Information

Kita *et al*. 10.1073/pnas.0804054105

SI Materials and Methods

Electroretinogram. Intravitreal injections of vehicle or fasudil at a final concentration of 10 or 30 μM were performed on days 0, 1, 3, 5, and 7. Electroretinogram was then performed on day 28 as previously described (1). The responses were differentially amplified (0.8–1,200 Hz), averaged, and recorded. Responses to 50 successive flashes presented at a rate of 2 Hz were averaged. The amplitude of the b-wave was measured from the cornea-negative to the -positive peak. The b-wave implicit time represents the interval from flash onset to the b-wave peak. The mean amplitude and latency of 2-Hz b-waves were then analyzed.

Stereoscopic, Light, and Transmission Electron Microscopy. The enucleated eyes were fixed in 4% paraformaldehyde. Whole eyes were cut along the vertical meridian and were examined by steremicroscopy (SMZ1500, Nikon). Paraffin-embedded sections were stained with H&E and examined by light microscopy. For transmission EM, the posterior segments of the eyes were fixed in 1% glutaraldehyde and 1% paraformaldehyde. The specimens were postfixed in veronal acetate buffer osmium tetroxide (2%), dehydrated in ethanol and water, and embedded in Epon. Ultrathin sections were cut from blocks and mounted on copper grids. The specimens were examined with an electron microscope (H7650, Hitachi, Japan).

TUNEL. Four micrometer-thick sections were made from samples fixed in 4% paraformaldehyde and embedded in paraffin. TUNEL staining was performed with the TdT Fluorescein *in Situ* Apoptosis Detection Kit (R&D Systems) according to the manufacturer's protocol. The sections were costained with propidium iodide (Molecular Probes, Eugene, OR) to observe the cell nuclei under a fluorescence microscope (BIOREVO BZ-9000, KEYENCE, Japan). As a TUNEL positive control, we used the retina of rabbit PVR model.

Cell Count. Rabbit conjunctival fibroblasts were seeded sparsely (1×10^4/well) in collagen coated 12-well plates and stimulated 3 days with DMEM containing 10% FBS with or without fasudil at 10 or 30 μM concentrations to evaluate the effect of fasudil on serum-induced fibroblast proliferation. The cells were collected and the number of cells was counted by Z1 Coulter cell and particle counter (Beckman Coulter, Fullerton, CA). To evaluate the effect of fasudil on apoptosis, subconfluent fibroblasts had been stimulated with serum free DMEM or rabbit vitreous with or without fasudil for 3 days and the number of cells was counted.

1. Ito S, *et al.* (1999) The effect of tranilast on experimental proliferative vitreoretinopathy. *Graefes Arch Clin Exp Ophthalmol* 237:691–696.

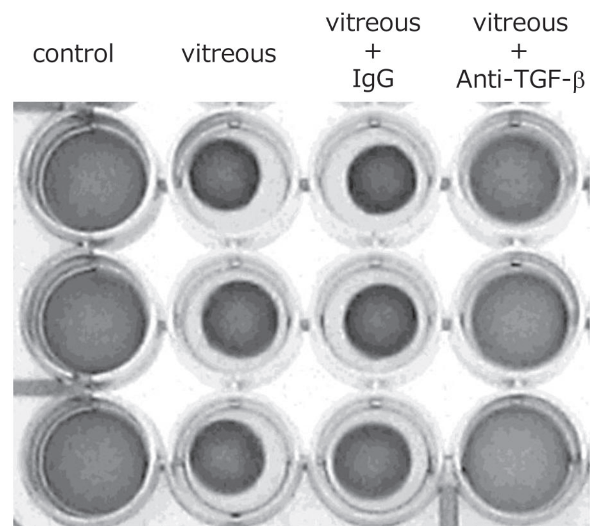

Fig. S1. Mouse control IgG does not suppress the vitreous-induced collagen gel contraction.

PNAS PNAS PNAS PNAS PNAS

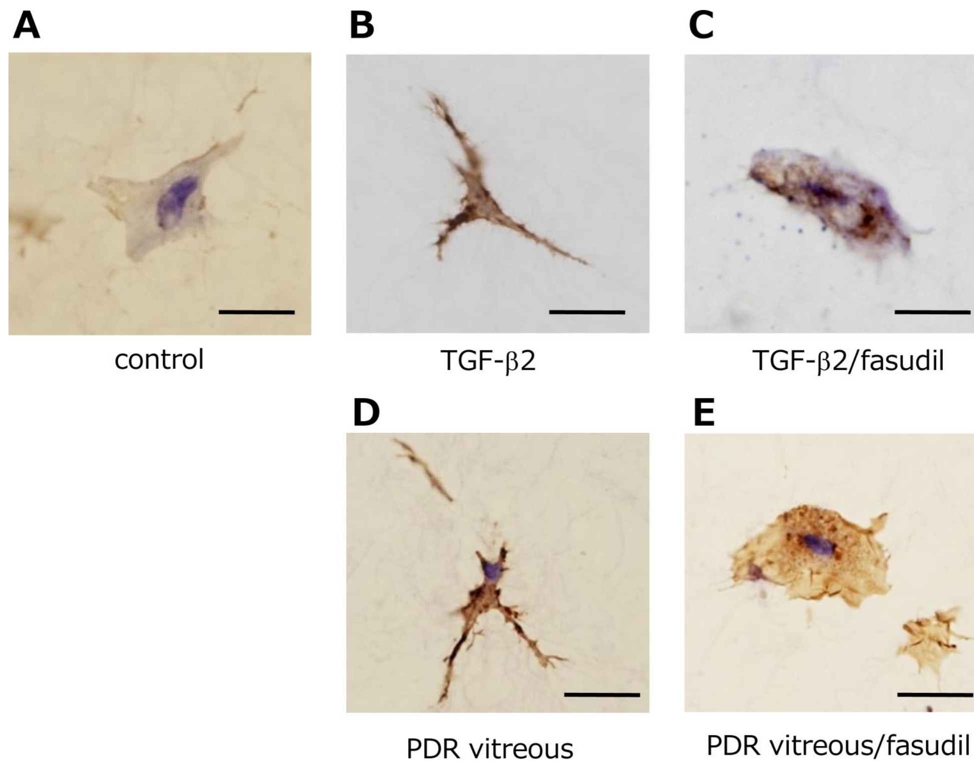

Fig. S2. Immunohistochemical analysis of α-SMA (brown) by hyalocytes embedded in collagen gels. Representative micrographs, showing hyalocyte-containing collagen gels that were treated with control (DMEM) (*A*), recombinant TGF-β2 (*B*), recombinant TGF-β2 with fasudil (20 μM) (*C*), PDR/PVR vitreous (*D*), and PDR/PVR vitreous with fasudil (20 μM) (*E*). (Scale bars, 10 μm.)

Fig. S3. Concentrations of TGF-βs in the vitreous with *in vivo* experimental PVR. Concentrations of total TGF-β1 (*A*) or TGF-β2 (*B*) and activated TGF-β2 (*C*) in the rabbit vitreous were measured by ELISA. Activated TGF-β1 was undetectable in each vitreal sample. *, $P < 0.05$ vs. control.

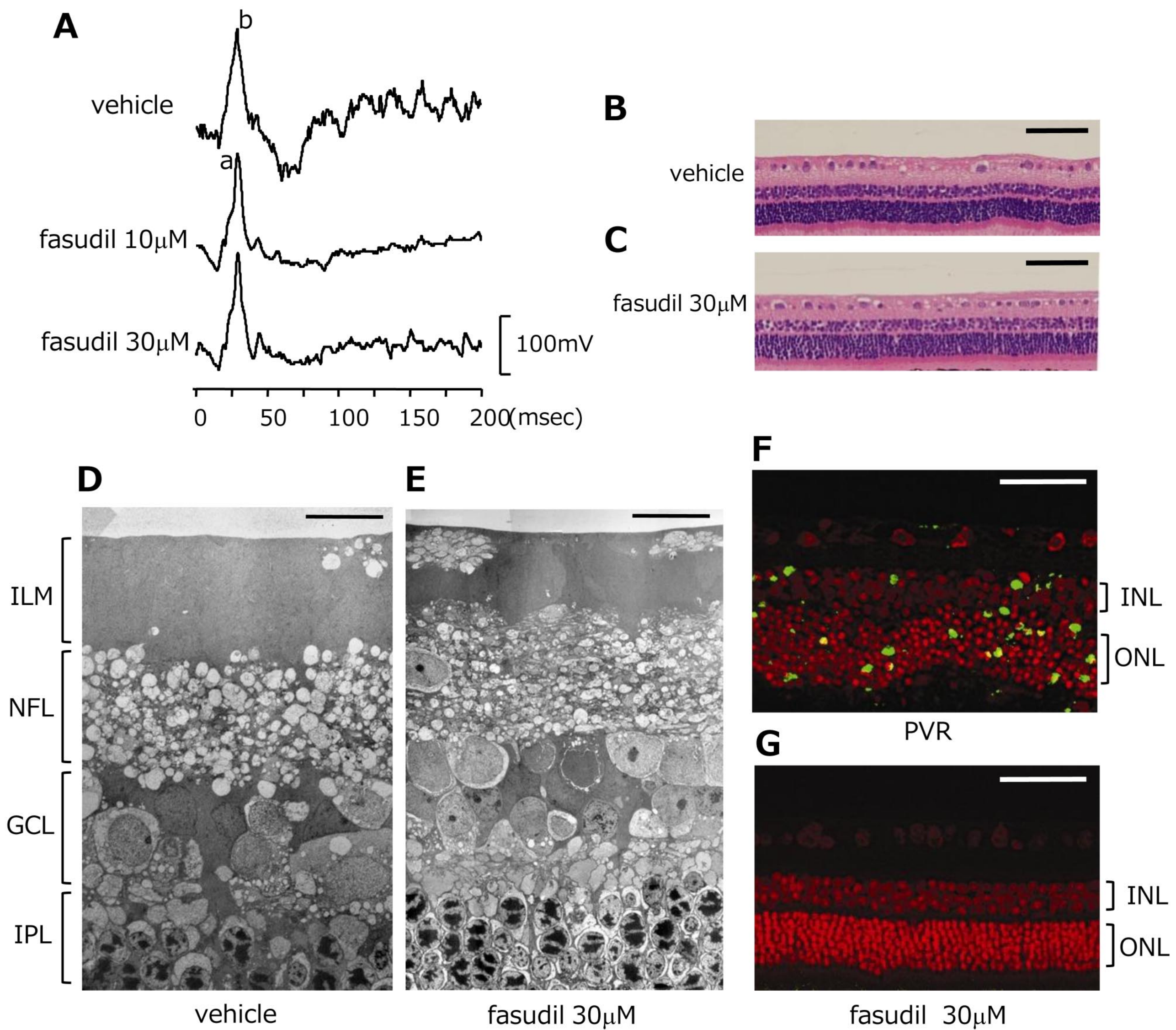

Fig. S4. Physiological and histological examinations of rabbit eyes injected with fasudil. (*A*) Vehicle or fasudil was intravitreally injected at days 0, 1, 3, 5, and 7. Electroretinograms were obtained from rabbits in vehicle (*Top*), fasudil at 10 μM (*Middle*), and fasudil at 30 μM (*Bottom*) groups on day 28. Cornea-negative peak (*a*) and -positive peak (*b*). Retinal toxicity of intravitreal injection of fasudil (30 μM) was examined by light microscopy (*B* and *C*) (Scale bars, 100 μm.) and transmission EM (*D* and *E*) (Scale bars, 10 μm.). Whereas TUNEL positive cells (green) were observed in the external granular layer of the detached retina with PVR (*F*) (Scale bar, 50 μm.), as a positive control, no TUNEL positive cells were observed in the eyes treated with fasudil at 30 μM (*G*) (Scale bar, 50 μm.). ILM, internal limiting membrane; NFL, nerve fiber layer; GCL, ganglion cell layer; IPL, inner plexiform layer; INL, inner nuclear layer; ONL, outer nuclear layer

Fig. S5. Physiological and histological examinations of rat eyes injected with fasudil. (*A*) Vehicle or fasudil was intravitreally injected and electroretinograms were obtained from rats in vehicle (*Top*), fasudil at 10 μM (*Middle*), and fasudil at 100 μM (*Bottom*) groups 4 days after injection. Cornea-negative peak (*a*) and -positive peak (*b*). (*B*) Retinal toxicity of intravitreal injection of fasudil (10 μM and 100 μM) was examined by light microscopy. (Scale bars, 100 μm.)

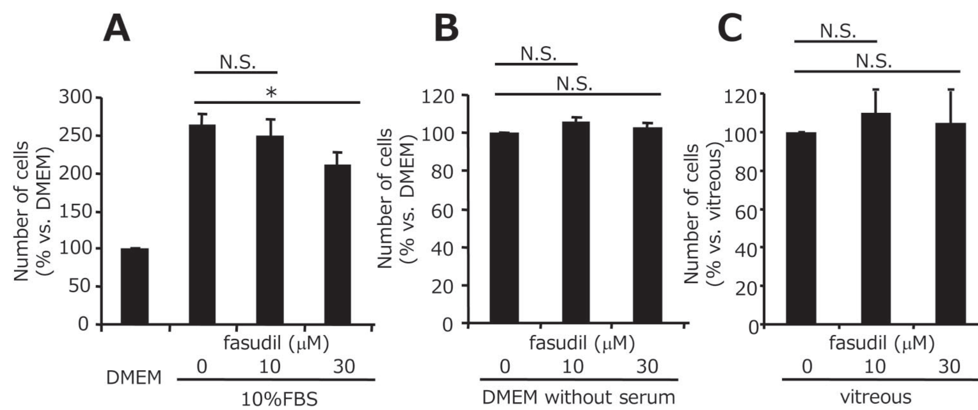

Fig. S6. Effects of fasudil on proliferation and apoptosis of rabbit conjunctival fibroblasts *in vitro*. (*A*) Effects of fasudil on serum-induced proliferation of fibroblasts. The cells were stimulated with serum-free DMEM or DMEM containing 10% FBS in the presence or absence of fasudil (10 or 30 μM) for 3 days. Cell numbers were counted and expressed as percentages of cell numbers in serum free DMEM. (*B*) Effects of fasudil on starvation-induced apoptosis of fibroblasts. The subconfluent cells were incubated with serum-free DMEM with or without fasudil (10 or 30 μM) for 3 days, and the number of cells was counted and expressed as percentages of cell numbers in DMEM. (*C*) Fibroblasts were stimulated with undiluted rabbit vitreous fluid with or without fasudil (10 or 30 μM) for 3 days and the number of cells was counted. *, $P < 0.05$; NS, not significant.

A

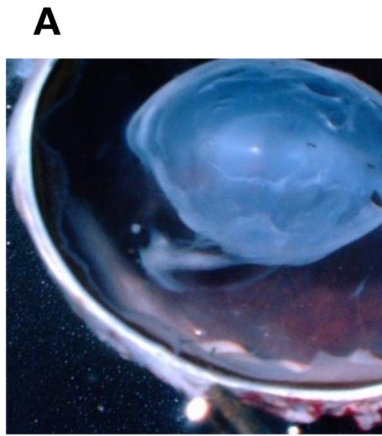

stage 1

B

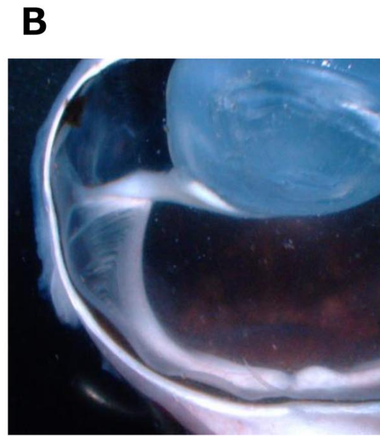

stage 3

C

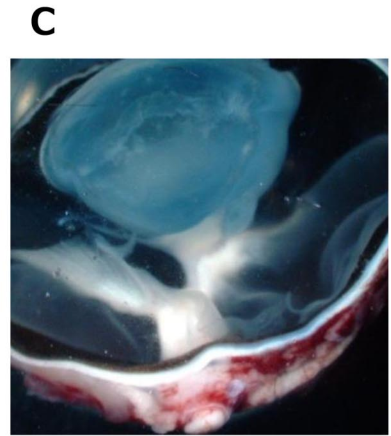

stage 4

Fig. S7. Stereoscopic images of each stage of experimental PVR. (*A*) Stage 1. (*B*) Stage 3. (*C*) Stage 4. Images of stage 2 and stage 5 are in Fig. 6 *B* and *C*, respectively.

Table S1. PVR stages

Stage	Characteristics
0	Normal eye
1	Intravitreal membrane
2	Focal traction
	Localized vascular changes, hyperemia, engorgement, dilation, blood vessel elevation
3	Localized detachment of medullary ray
4	Extensive retinal detachment
	Total medullary ray detachment, peripapillary retinal detachment
5	Total retinal detachment

PNAS PNAS PNAS PNAS PNAS